

Dimers of Dipyrrrometheneboron Difluoride (BODIPY) with Light Spectroscopic Applications in Chemistry and Biology

Fredrik Bergström,[†] Ilya Mikhalyov,^{†,‡} Peter Hägglöf,[§] Rüdiger Wortmann,[‡]
Tor Ny,[§] and Lennart B.-Å. Johansson^{*†}

Contribution from the Department of Chemistry, Biophysical Chemistry, Umeå University, S-901 87 Umeå, Sweden, Department of Medical Biosciences, Medical Biochemistry, Umeå University, S-901 87 Umeå, Sweden, and Physikalische Chemie, Universität Kaiserslautern, Erwin-Schrödinger-Strasse, D-67663 Kaiserslautern, Germany

Received April 17, 2001

Abstract: A ground-state dimer (denoted D_I) exhibiting a strong absorption maximum at 477 nm ($\epsilon = 97\,000\text{ M}^{-1}\text{cm}^{-1}$) can form between adjacent BODIPY groups attached to mutant forms of the protein, plasminogen activator inhibitor type 1 (PAI-1). No fluorescence from excited D_I was detected. A locally high concentration of BODIPY groups was also achieved by doping lipid phases (micelles, vesicles) with BODIPY-labeled lipids. In addition to an absorption band located at about 480 nm, a new weak absorption band is also observed at ca. 570 nm. Both bands are ascribed to the formation of BODIPY dimers of different conformation (D_I and D_{II}). Contrary to D_I in PAI-1, the D_{II} aggregates absorbing at 570 nm are emitting light observed as a broad band centered at about 630 nm. The integrated absorption band of D_I is about twice that of the monomer, which is compatible with exciton coupling within a dimer. The Förster radius of electronic energy transfer between a BODIPY excited monomer and the ground-state dimer (D_I) is $57 \pm 2\text{ \AA}$. A simple model of exciton coupling suggests that in D_I two BODIPY groups are stacked on top of each other in a sandwich-like configuration with parallel electronic transition dipoles. For D_{II} the model suggests that the $S_0 \rightarrow S_1$ transition dipoles are collinear. An explanation for the previously reported (*J. Am. Chem. Soc.* **1994**, *116*, 7801) exceptional light spectroscopic properties of BODIPY is also presented. These are ascribed to the extraordinary electric properties of the BODIPY chromophore. First, changes of the permanent electric dipole moment ($\Delta\mu \approx -0.05\text{ D}$) and polarizability ($-26 \times 10^{-40}\text{ C m}^2\text{ V}^{-1}$) between the ground and the first excited states are small. Second, the $S_0 \leftrightarrow S_1$ electronic transition dipole moments are perpendicular to $\Delta\vec{\mu}$.

Introduction

An increasing number of publications report on various applications of BODIPY (4,4-difluoro-4-borata-3a-azonia-4a-aza-s-indacene) and derivatives thereof.^{1–7} One important reason

for this is the exceptional spectral and photophysical stability of BODIPY,⁸ as compared to other fluorescent groups. For example, the commonly used fluorescein exhibits a very similar spectral range as BODIPY, while contrary to BODIPY, the fluorescence and absorption spectra, as well as the fluorescence lifetime, are sensitive to pH and polarity. These remarkable properties of BODIPY have been valuable for developing a new method, the so-called DDEM method.^{9,10} This is based on monitoring donor–donor energy migration within a pair of chemically and photophysically identical groups. Hence, BODIPY groups have proved to be useful in studies aimed at exploring protein structure.^{11,12} To explain the remarkable properties of BODIPY, electrooptical absorption measurements (EOAM) were performed. These experiments provide values on electric properties of the BODIPY chromophore, like the

* Corresponding author. Fax: +46-90-7867779. E-mail: Lennart.Johansson@chem.umu.se.

[†] Department of Chemistry, Biophysical Chemistry, Umeå University.

[‡] Permanent Address: Shemyakin & Ovchinnikov Institute of Bioorganic Chemistry, Russian Academy of Sciences, ul. Miklukho-Maklaya 16/10, Moscow 117871, Russia.

[§] Department of Medical Biosciences, Medical Biochemistry, Umeå University.

[‡] Universität Kaiserslautern.

- (1) Haugland, R. P. *Handbook of Fluorescent Probes and Research Chemicals*, 6th ed.; Molecular Probes: Eugene, OR, 1996.
- (2) Hung, S.-C.; Mathies, R. M.; Glazer, A. N. *Anal. Biochem.* **1997**, *252*, 78–88.
- (3) Kawahara, S.-I.; Uchimaru, T.; Murata, S. *Chem. Commun.* **1999**, 563–564.
- (4) Lee, L. G.; Spurgeon, S. L.; Heiner, C. R.; Benson, S. C.; Rosenblum, B. B.; Menchen, S. M.; Graham, R. J.; Constantinescu, A.; Upadhyay, K. G.; Cassel, J. M. *Nucleic Acids Res.* **1997**, *25*, 2816–2822.
- (5) Bergström, F.; Hägglöf, P.; Karolin, J.; Ny, T.; Johansson, L. B.-Å. *Proc. Natl. Acad. Sci.* **1999**, *96*, 12477–12481.
- (6) Burghart, A.; Kim, H.; Welch, M. B.; Thoresen, L. H.; Reibenspies, K.; Burgess, K.; Bergström, F.; Johansson, L. B.-Å. *J. Org. Chem.* **1999**, *64*, 7813–7819.
- (7) Burghart, A.; Thoresen, L. H.; Chen, J.; Burgess, K.; Bergström, F.; Johansson, L. B.-Å. *Chem. Commun.* **2000**, 2203–2204.

- (8) Karolin, J.; Johansson, L. B.-Å.; Strandberg, L.; Ny, T. *J. Am. Chem. Soc.* **1994**, *116*, 7801–7806.
- (9) Johansson, L. B.-Å.; Edman, P.; Westlund, P.-O. *J. Chem. Phys.* **1996**, *105*, 10896–10904.
- (10) Johansson, L. B.-Å.; Bergström, F.; Edman, P.; Grechishnikova, I. V.; Molotkovsky, J. G. *J. Chem. Soc., Faraday Trans.* **1996**, *92*, 1563–1567.
- (11) Karolin, J.; Fa, M.; Wilczynska, M.; Ny, T.; Johansson, L. B.-Å. *Biophys. J.* **1998**, *74*, 11–21.
- (12) Fa, M.; Bergström, F.; Hägglöf, P.; Wilczynska, M.; Johansson, L. B.-Å.; Ny, T. *Structure* **2000**, *8*, 397–405.

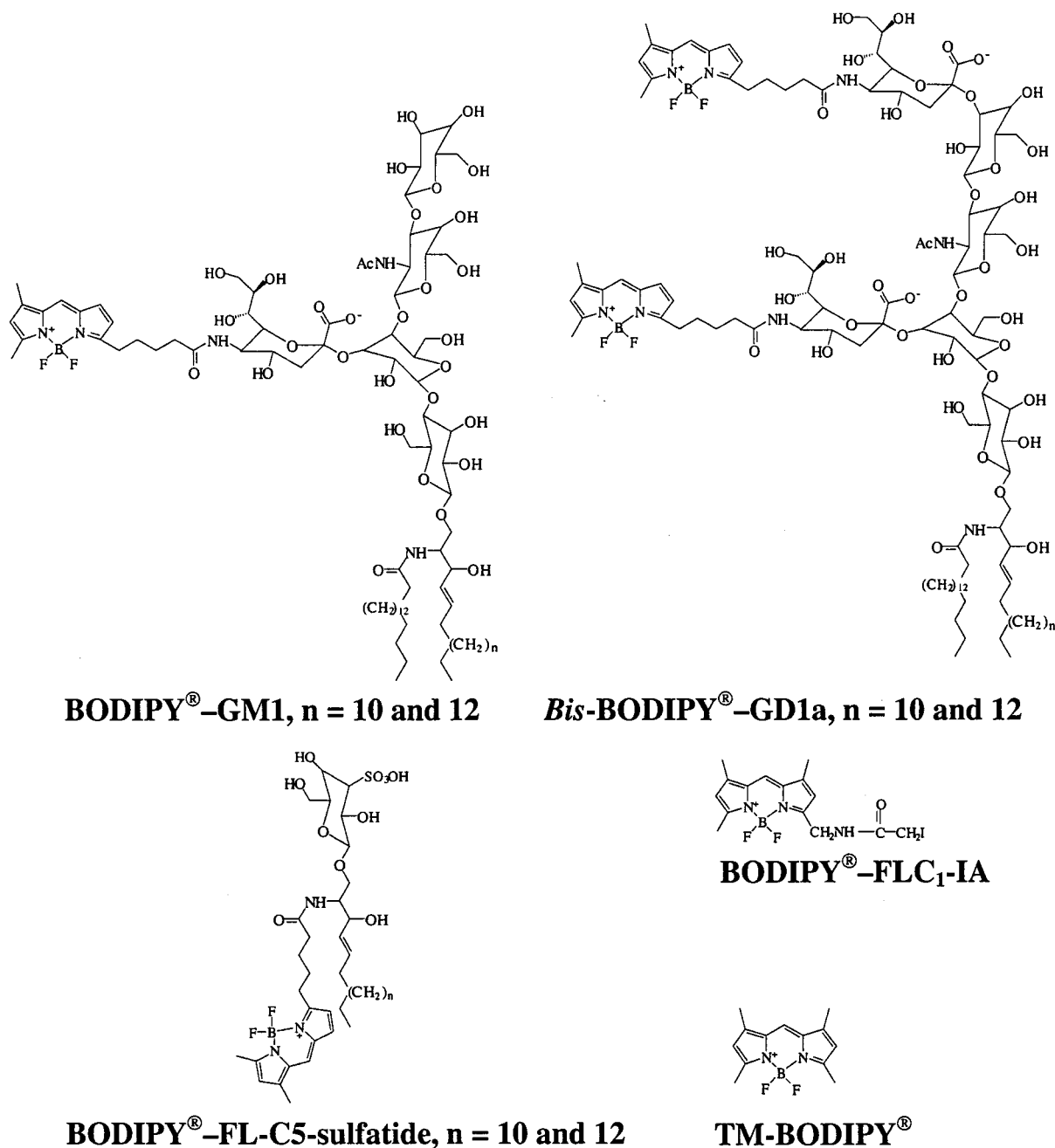


Figure 1. Structure formulas of 3,3',4,4'-difluoro-1,3,5,7-tetramethyl-4a-aza-s-indacene (TM-BODIPY) and the sulfhydryl specific BODIPY used for labeling of cystein residues in proteins (FLC₁IA BODIPY). The lipid structures are two BODIPY-labeled gangliosides GM1 GD1a, and a monolabeled BODIPY-FL-C5-sulfatide.

electric permanent dipole moments and polarizabilities of the ground and excited states. In addition to understanding solvent-solute interaction, electrooptical information may also provide an insight into aggregation of BODIPY that occurs at locally high concentrations.

Little is still known about aggregation and the properties of aggregated BODIPY. Pagano and Chen¹³ reported the fluorescence spectrum of a BODIPY-labeled sphingolipid in lipid vesicles that shows a red emission band (centered at about 630 nm), in addition to the normal green emission (peak at 515 nm). They propose excimer formation to be the reason for the red emission. As is shown by the present study, this is not the case.

In present work BODIPY-BODIPY interaction is explored by investigating systems with a microscopically high, but macroscopically low concentration of BODIPY. For this lipid vesicles were prepared containing BODIPY-labeled gangliosides (Figure 1). Furthermore, experiments were performed with BODIPY attached to two nearby thiol groups in mutants of plasminogen activator type 1 (PAI-1).¹⁴ A dimer thereby formed can be useful in probing short distances between specific regions in proteins, for example in studies of protein folding. Previously, sulfhydryl-specific derivatives of pyrene were used¹⁵⁻¹⁷ for this

(13) Pagano, R. E.; Chen, C.-S. *Ann. N.Y. Acad. Sci.* **1998**, *845*, 152-160.

(14) Wilczynska, M.; Fa, M.; Karolin, J.; Ohlsson, P.-I.; Johansson, L. B.-Å.; Ny, T. *Nat. Struct. Biol.* **1997**, *4*, 354-356.

(15) Betcher-Lange, S.; Lehrer, S. S. *J. Biol. Chem.* **1978**, *253*, 3757-3760.

(16) Jung, K.; Jung, H.; Wu, J.; Privé, G. G.; Kaback, R. H. *Biochemistry* **1993**, *32*, 12273-12278.

purpose. In the excited state a hydrophobic pyrene molecule forms a dimer with a ground-state pyrene, provided suitable orbital contact between them is achieved. Because this excimer (excited state dimer) exhibits a different fluorescence emission, molecular contact is confirmed. In other reports rhodamine dyes were shown to form dimers.^{18,19} Energy transfer between Rhodamine groups and dimers thereof was also recently used to study the aggregation of hydrophobic transmembrane peptides²⁰ and lipid membrane fusion.²¹ Dimers of BODIPY could be used for similar purposes, whereby BODIPY enables localization to more polar regions. Another field of application might be for characterizing microconfinements, such as the aggregate size of micelles and similar structures formed by amphiphiles.^{22,23} Finally, dimers of BODIPY may serve as functional units in supramolecular systems.²⁴

Materials and Methods

1,2-Dioleoyl-*sn*-glycero-3-phosphocholine (DOPC) was purchased from Avanti Polar Lipids, Inc. (Pelham, AL), Tris-base and DEAE-Sephadex A-25 were purchased from Sigma Chemical Co. (St. Louis, MO), sulfatide from bovine brain was purchased from Matreya, Inc. (Pleasant Gap, PA), and BODIPY-FL-C₁-IA and TM-BODIPY (Figure 1) were purchased from Molecular Probes, Inc. (Eugene, OR). Tetramethylammonium hydroxide, isobutyl chloroformate, and triethylamine were purchased from Fluka (Switzerland). Silica gel 60 and 100 (63–200 μm) were purchased from Merck GmbH (Darmstadt, Germany). All solvents used were reagent grade and freshly distilled. Gangliosides GM1 and GD1a were isolated from bovine brain, as described by Svennerholm,²⁵ and purified by DEAE-Sephadex A-25 column chromatography²⁶ and silica gel 100 column chromatography.

Expression and Labeling of PAI-1 Cys-Mutants. The construction of PAI-1 Cys-double mutant S344C-M347C has been described previously.²⁷ The mutant protein was expressed in *E. coli* strain SG20043 *lon*⁻ and was purified to homogeneity as described.²⁸ The inhibitor activity was determined by a chromogenic assay and by complex formation with urokinase type plasminogen activator (uPA).²⁹ Labeling of PAI-1 cysteine double mutant S344C-M347C was performed as described elsewhere,¹² except that Tween was omitted from the chromatography buffer. The labeling efficiency varied between 25 and 80 mol %. The degree of labeling was obtained from the absorption spectra of BODIPY and the protein. Samples were measured in both the absence and presence of (50% v/v) glycerol.

Preparation of Vesicles. The vesicles were prepared by the extrusion technique³⁰ by using an extruder manufactured by Lipex Biomembranes Inc. (Vancouver, Canada). Briefly, the dried lipid film, containing DOPC and probe, was hydrated to the necessary concentration by 20 mM Tris-HCl buffer (pH 7.4), containing 1 mM disodium salt of EDTA.

This mixture was freeze–thawed five times and then passed 10 times through two polycarbonate filters (Nucleopore) with a pore size of 100 nm.

Syntheses. In all procedures described below, the fluorescent substances were protected for exposure of light.

N-(BODIPY-FL-pentanoyl)-galactosylcerebroside-sulfate (BODIPY-Sulfatide) was synthesized from *lyso*-sulfatide by *N*-acylation. *lyso*-Sulfatide was obtained by alkaline hydrolysis of a natural sulfatide as described earlier.³¹ *N*-Acylation was carried out with an *N*-succinimidyl ester of BODIPY-FL-pentanoic acid by a method previously described by Viani et al.³² In brief, 10 μmol of *lyso*-sulfatide was dissolved in 2 mL of THF–water, 9:1, then 15 μmol of triethylamine and 15 μmol of *N*-succinimidyl ester of BODIPY-FL-pentanoic acid were added. The reaction mixture was stirred at room temperature overnight and, after evaporation of solvents, purified by column chromatography on silica gel 60 in chloroform–methanol–water, 80:10:1 (v/v/v). This yielded, as a red powder, 3.4 μmol (34 mol %) of the BODIPY-sulfatide. The purity was better than 99%, as revealed by HPTLC. R_f = 0.48 in chloroform–methanol–2.5 M aqueous NH₃, 65:25:4 (v/v/v), which is comparable to the value of natural sulfatide (R_f = 0.56).

N-(BODIPY-FL-pentanoyl)-neuraminosyl-ganglioside GM1 (BODIPY-GM1) was synthesized from de-acetyl-ganglioside GM1 by *N*-acylation. The de-acetyl-ganglioside GM1 was obtained by alkaline hydrolysis as is described by Sonnino et al.,³³ when using 1 M tetramethylammonium hydroxide in *n*-butanol–water, 9:1, at 100 °C. The de-acetyl-GM1 was *N*-acylated by using a mixed anhydride.³⁴ In brief, 10 μmol of BODIPY-FL-pentanoic acid was dissolved in dried chloroform, and 10 μmol of triethylamine and 10 μmol of isobutylchloroformate were then added. The reaction mixture was stirred for 1 h at room temperature. After evaporation, it was dissolved in 3 mL of ethyl acetate, washed with 2 mL of water (saturated with NaCl), and finally stored for 2 h over anhydrous sodium sulfate. The solution of the anhydride of BODIPY-FL-pentanoic acid was evaporated and dissolved in 1 mL of THF. This was added to a solution of 4 μmol of de-acetyl-GM1 dissolved in 2 mL of THF–water (at the ratio of 10:1) with 5 μmol of triethylamine and the reaction mixture was run under stirring overnight at room temperature. BODIPY-GM1 was isolated and purified by using silica gel 100 column chromatography with chloroform–methanol–water, 65:25:2 (v/v/v), as the eluent. The fractions containing the fluorescent and resorcinol-positive product were collected. The final yield of BODIPY-GM1 was 1.2 μmol (corresponding to 30 mol %), obtained as a red powder. The purity was better than 99% as judged by HPTLC. The R_f value was 0.45 in chloroform–methanol–15 mM aqueous CaCl₂, 60:35:8 (v/v/v), while it was 0.26 for nonlabeled GM1. ¹H NMR (CD₃OD) δ 2.44 (s, 3H), 2.66 (s, 3H), 4.46 (d, J = 8 Hz, 1H), 4.57 (d, J = 8 Hz, 1H), 4.60 (d, J = 8 Hz, 1H), 5.08 (d, J = 8 Hz, 1H), 5.61 (m, J = 8 Hz, 1H), 5.84 (m, J = 8 Hz, 1H), 6.34 (s, 1H), 6.53 (d, J = 4 Hz, 1H), 7.19 (d, J = 4 Hz, 1H), 7.56 (s, 1H). In conclusion, BODIPY-GM1 contains one BODIPY-FL-C5-residue per GM1 molecule.

Di-[*N*-(BODIPY-FL-pentanoyl)-neuraminosyl]-ganglioside GD1a (*bis*-BODIPY-GD1a) was synthesized from the di-(de-acetyl)-ganglioside GD1a and purified in analogy to BODIPY-GM1. Briefly, bis-BODIPY-GD1a was obtained as a red powder from 2 μmol of di-(de-acetyl)-GD1a and 10 μmol of BODIPY-FL-pentanoic acid. The yield was 0.7 μmol (35 mol %) and the purity better than 99%, as revealed by HPTLC. The R_f value was 0.48 in chloroform–methanol–15 mM aqueous CaCl₂, 60:35:8 (v/v/v), as compared to 0.16 for the nonlabeled

- (17) Hammarström, P.; Kalman, B.; Jonsson, B.-H.; Carlsson, U. *FEBS Lett.* **1997**, *420*, 63–68.
 (18) Penzkofer, A.; Lu, Y. *Chem. Phys.* **1986**, *103*, 399.
 (19) Gál, M. E.; Kelly, G. R.; Kurucsev, T. *J. Chem. Soc., Faraday Trans. 2* **1973**, *69*, 395–402.
 (20) Bogen, S.-T.; de Korte-Kool, G.; Lindblom, G.; Johansson, L. B.-Å. *J. Phys. Chem. B* **1999**, *103*, 8344–8352.
 (21) Hoekstra, D.; Boes, T. D.; Klappe, K.; Wilschut, J. *Biochemistry* **1984**, *23*, 5675.
 (22) Tachiya, M. *Chem. Phys. Lett.* **1975**, *33*, 289–292.
 (23) Almgren, M.; Löfroth, J.-E. *J. Chem. Phys.* **1982**, *76*, 2734–2743.
 (24) Balzani, V.; Scandola, F. *Supramolecular Photochemistry*; Chichester, UK, 1991.
 (25) Svennerholm, N. *Methods in Carbohydrate Chemistry*; Whistler, R. L. Ed.; Academic Press: New York, 1973; pp 464–474.
 (26) Momoi, T.; Ando, S.; Nagai, Y. *Biochim. Biophys. Acta* **1976**, *441*, 488–497.
 (27) Aleshkov, S. B.; Fa, M.; Karolin, J.; Strandberg, L.; Johansson, L. B.-Å.; Wilczynska, M.; Ny, T. *J. Biol. Chem.* **1996**, *271*, 21231–21238.
 (28) Kwassman, J.-O.; Shore, J. D. *Fibrinolysis* **1995**, *9*, 215–221.
 (29) Lawrence, D.; Strandberg, L.; Grundström, T.; Ny, T. *Eur. J. Biochem.* **1989**, *186*, 523–533.

- (30) Hope, M. Y.; Bally, M. B.; Cullis, P. R. *Biochim. Biophys. Acta* **1985**, *812*, 55.
 (31) Dubois, G.; Zalc, B.; Saux, F.; Baumann, N. *Anal. Biochem.* **1980**, *102*, 313–317.
 (32) Viani, P.; Galimberti, C.; Marchesini, S.; Gervato, G.; Cestaro, B. *Chem. Phys. Lipids* **1988**, *46*, 89–97.
 (33) Sonnino, S.; Kirschner, G.; Ghidoni, R.; Acquotti, D.; Tettamanti, G. *J. Lipid Res.* **1985**, *26*, 248–257.
 (34) Acquotti, D.; Sonnino, S.; Masserini, M.; Gasella, L.; Fronza, G.; Tettamanti, G. *Chem. Phys. Lipids* **1986**, *40*, 71–86.

GD1a. $^1\text{H NMR}$ (CD_3OD) δ 2.44 (s, 6H), 2.66 (s, 6H), 4.46 (d, $J = 8$ Hz, 1H), 4.57 (d, $J = 8$ Hz, 1H), 4.60 (d, $J = 8$ Hz, 1H), 5.08 (d, $J = 8$ Hz, 1H), 5.61 (m, $J = 8$ Hz, 1H), 5.84 (m, $J = 8$ Hz, 1H), 6.34 (s, 2H), 6.53 (d, $J = 4$ Hz, 2H), 7.19 (d, $J = 4$ Hz, 2H), 7.56 (s, 2H). In conclusion, BODIPY-GD1a contains two BODIPY-FL-C5-residues per GD1a molecule.

Fluorescence and Absorption Spectra. The fluorescence spectra were recorded on a SPEX Fluorolog 112 (SPEX Ind., NJ) equipped with Glan-Thompson polarizers. The spectral bandwidths were 5.5 and 2.7 nm for the excitation and emission monochromators, respectively. The fluorescence spectra were corrected. To calibrate the spectrometer, a standard lamp from the Swedish National Testing and Research Institute (Borås, Sweden) was used. Absorption spectra were recorded on a GBC 920 spectrophotometer (GBC, Inc., Australia).

Calculating the Förster Radius between Monomeric and Dimeric BODIPY. The absorption spectrum of the dimer and the corrected fluorescence spectrum of the monomeric BODIPY were carefully determined. With use of these data, the Förster radius (R_0) was calculated from

$$R_0 = \left\{ \frac{9000(\ln 10) \langle \kappa^2 \rangle \Phi J}{128\pi^2 n^4 N_A} \right\}^{1/6}$$

$$J = \int_{\text{band}} \epsilon(\tilde{\nu}) f(\tilde{\nu}) \tilde{\nu}^{-4} d\tilde{\nu}$$

$$f(\tilde{\nu}) = \frac{F(\tilde{\nu})}{\int F(\tilde{\nu}) d\tilde{\nu}} \quad (1)$$

Here $F(\tilde{\nu})$, $\tilde{\nu}$, $\epsilon(\tilde{\nu})$, Φ , and N_A denote the corrected fluorescence spectrum, the wavenumber of light (cm^{-1}), the molar absorptivity of the acceptor, and the fluorescence quantum yield of the donor and the Avogadro constant, respectively. In the calculations $\Phi = 0.92$,^{8,35} and $\langle \kappa^2 \rangle = 2/3$ is used as a reference state. The refractive index $n = 1.4$ was used in calculating R_0 . For electronic energy transfer from monomeric BODIPY to its dimer, a value of $R_0 = 57 \pm 2 \text{ \AA}$ was obtained for the PAI-1 and the lipid (BODIPY-sulfatide) system.

Time-Correlated Single Photon Counting (TCSPC). Fluorescence lifetime decays were measured with an instrument from IBH Consultants Ltd (Glasgow, Scotland) equipped with dichroic sheet polarizers. The instrument uses a pulsed light emitting diode (LED) operating at a repetition rate of ca. 800 kHz. The excitation and emission wavelengths were selected by monochromators combined with interference filters centered at 500 and 550 nm, respectively. Fluorescence lifetime decays were measured with the emission polarizer set at the magic angle (54.7°) relative to the excitation polarizer. The instrumental response function, $I(t)$, was determined by using a light-scattering solution. The experimental fluorescence decay ($F(t)$) is a convolution between the true decay of the photophysics $\{f(t)\}$ and $I(t)$, i.e.

$$F(t) = \int_0^t I(t - \gamma) f(\gamma) d\gamma \quad (2)$$

The photophysics was modeled as a sum of exponential functions,

$$f(t) = \sum_{i=1}^2 a_i \exp(-t/\tau_i) \quad (3)$$

and deconvoluted by using a nonlinear least-squares analysis, based on the Levenberg–Marquardt algorithm.^{36,37} The average fluorescence lifetime ($\langle \tau \rangle$) was calculated from

$$\langle \tau \rangle = \frac{\sum_{i=1}^2 a_i \tau_i^2}{\sum_{i=1}^2 a_i \tau_i} \quad (4)$$

In eq 4, τ_i stands for the i th fluorescence lifetime component of a multiexponential fluorescence decay.

Electrooptical Absorption Measurements (EOAM). EOAM spectra were recorded in dioxane at 298 K. The solvent was purified as previously described³⁸ and carefully dried by distillation from Na/K under Ar atmosphere prior to use. Details of the EOAM apparatus are given elsewhere.³⁹

In an electrooptical absorption experiment^{40,41} one observes the effect of an externally applied electric field (E) on the absorbance of a dilute solution of a chromophore in an inert solvent. The change of absorbance is related to the change of the molar decadic absorption coefficient $\{\epsilon(\tilde{\nu})\}$ induced by the field and is described by the function⁴⁰

$$L(\phi, \tilde{\nu}) = (1/|E|^2) [\epsilon^{|E|}(\phi, \tilde{\nu}) - \epsilon(\tilde{\nu})] / \epsilon(\tilde{\nu}) \quad (5)$$

Here $\epsilon(\tilde{\nu})$ and $\epsilon^{|E|}(\tilde{\nu})$ denote the molar absorption coefficient at the wavenumber $\tilde{\nu}$ in the absence and presence of the applied electrical field, respectively. The angle ϕ denotes the angle between the direction of E and the electric field vector of incident linearly polarized light. Usually, $L(\phi, \tilde{\nu})$ is measured at two orientations, namely for $\phi = 0^\circ$ and 90° , and many different wavenumbers in the absorption band. The EOAM spectrum is then represented in the form of $L(\phi, \tilde{\nu})\epsilon(\tilde{\nu})/\tilde{\nu}$ and analyzed by multilinear regression, in terms of $\epsilon(\tilde{\nu})/\tilde{\nu}$ and its first and second derivative. The regression yields a set of six coefficients denoted D , E , ..., I .⁴⁰ Within the present work, only the following coefficients are significant:

$$E = \left(\frac{1}{kT}\right)^2 [3(\hat{m} \cdot \mu) - \mu^2] + \frac{1}{kT} [3(\hat{m} \cdot \alpha \cdot \hat{m}) - \text{Tr} \alpha] \quad (6)$$

$$F = \frac{1}{kT} (\mu \cdot \Delta\mu) + \frac{1}{2} \text{Tr} \Delta\alpha \quad (7)$$

$$G = \frac{1}{kT} (\hat{m} \cdot \mu)(\hat{m} \cdot \Delta\mu) + \frac{1}{2} (\hat{m} \cdot \alpha \cdot \hat{m}) \quad (8)$$

In eqs 6–8 \hat{m} is the unit vector of the transition dipole in a molecule-fixed frame, and μ and α denote the permanent dipole moment and the static polarizability tensor of the electronic ground state, respectively. In analogy, $\Delta\mu$ and $\Delta\alpha$ stand for the change of the dipole moment and the polarizability upon excitation to the Franck–Condon (FC) excited state. Effects of the applied electric field on the magnitude of the transition dipole are described by the coefficient D experiment.⁴⁰ The D coefficient and a number of related terms are usually small, and were neglected in eqs 6–10. Likewise effects of the square of the dipole difference $\Delta\mu$, which enters in the coefficients H and I , are negligible. Local field corrections have to be carried out to account for differences between the macroscopically applied field and the local field. Complete expressions for such corrections are available⁴⁰ but were for simplicity omitted in eqs 6–10. In this paper we approximate the local field

(36) Demas, J. N. *Excited-state lifetime measurements*; Academic Press: New York, 1983.

(37) O'Connor, D. V.; Phillips, D. *Time-correlated Single Photon Counting*; Academic Press: London, 1984.

(38) Wortmann, R.; Krämer, R.; Galnia, C.; Lebus, S.; Detzer, N. *Chem. Phys.* **1993**, *173*, 99–108.

(39) Baumann, W. *Ber. Bunsen-Ges. Phys. Chem.* **1976**, *80*, 231.

(40) Liptay, W. *Dipole Moments and Polarizabilities of Molecules in Excited Electronic State*; Lim, E. C., Ed.; Academic Press: New York, 1974; Vol. 1, pp 129–229.

(41) Wortmann, R.; Elich, K.; Lebus, S.; Liptay, W.; Borowicz, P.; Grabowska, A. *J. Phys. Chem.* **1992**, *96*, 9724–9730.

(35) Johnson, I. D.; Kang, H. C.; Haugland, R. P. *Anal. Chem.* **1991**, *198*, 228–237.

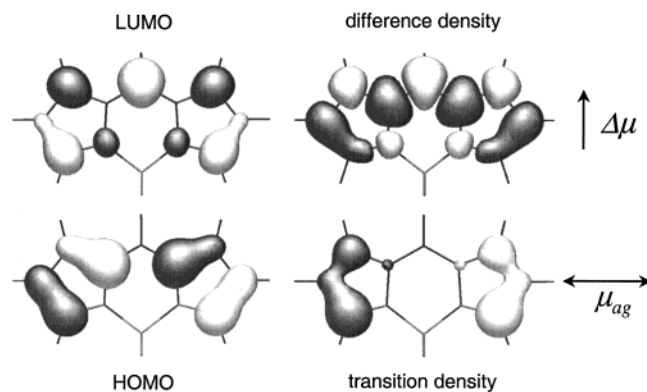


Figure 2. The calculated HOMO, LUMO, difference density, and transition density of TM-BODIPY. The CNDO/S method was used, assuming an AM1 optimized geometry.

corrections by the well-known Lorentz' factors $(\epsilon_r + 2)/3$, where ϵ_r stands for the relative permittivity of the solvent.

Nuclear Magnetic Resonance Spectroscopy. ^1H NMR (500 MHz) were recorded for final compounds in perdeuterated methanol at 300 K on a Bruker DRX-500 pulse spectrometer operating in the Fourier transform mode. The pulse width was 9 μs , the acquisition time was 1.3 s, and the number of transients was 128. The signals were assigned by putting the central signal of methanol at 3.47 ppm.

Results and Discussion

Electrooptical Absorption Measurements (EOAM) on TM-BODIPY. The absorption spectrum of BODIPY exhibits an intense $S_0 \rightarrow S_1$ transition with its maximum at 505 nm. This band has a small fwhm as well as a short Franck–Condon progression that is characteristic of the cyanine type of chromophores. The spectrum is also similar to the spectra of many merocyanine dyes being close to the cyanine limit.^{42–45} Besides, such dyes are found to be of interest as optimizing chromophores for organic photorefractive materials. For such a compact chromophore one should also notify the large value of the integrated absorption, which is proportional to the square of the transition dipole. This can be used to explore the electronic structure of BODIPY by means of semiempirical calculations (see Figure 2). Interestingly, the transition density shows large amplitudes at the ends of the chromophore with only one main node, leading to a large transition dipole (μ_{ag}). On the other hand, the dipole difference density ($\Delta\mu$) is alternating. As a consequence, only small differences in the dipole moment are expected and found (see Table 1). Taken together, these data explain the exceptionally weak influence from solvent polarity on the spectral properties of the BODIPY chromophore.

The quantitative evaluation of the EOAM spectra starts out with the ground-state dipole moment that can be determined from the electrooptical regression coefficient E (cf. eq 6). This coefficient captures the electrochromic effect due to reorientation of the molecules induced by the interaction of the ground-state dipole moment and—usually to a minor extent—of the anisot-

Table 1. Results of the Analysis of EOAM Data Determined for TM-BODIPY in Dioxane at 298 K^a

property	value extracted
E , 10^{-20} $\text{m}^2 \text{V}^{-2}$	-1515 ± 73
F , 10^{-40} $\text{C m}^2 \text{V}^{-1}$	-120 ± 11
G , 10^{-40} $\text{C m}^2 \text{V}^{-1}$	-26 ± 11
M , g mol^{-1}	248.08
λ_{ag} , nm	505
$\epsilon_{\text{max}}(\lambda_{\text{ag}})$, $\text{m}^2 \text{mol}^{-1}$	9384
$ \mu $, 10^{-30} C m	10.9 ± 0.3
$\Delta \mu $, 10^{-30} C m	-1.8 ± 0.2
$\Delta\alpha$, 10^{-40} $\text{C m}^2 \text{V}^{-1}$	-26 ± 11
μ_{ag} , 10^{-30} C m	22.9

^a The maximum of the molar absorptivity obtained for wavelength λ_{ag} in the $S_0 \rightarrow S_1$ transition band is denoted by $\epsilon_{\text{max}}(\lambda_{\text{ag}})$. The value of the electronic transition dipole moment is μ_{ag} while $|\mu|$ stands for the absolute value of the permanent electric dipole moment in the electronic ground state of BODIPY. The change of permanent dipole moment and anisotropic polarizability upon $S_0 \rightarrow S_1$ excitation are denoted $\Delta|\mu|$ and $\Delta|\alpha|$, respectively. The coefficients E – G are defined in the Materials and Methods section. Details for estimating errors are given in the paper by Liptay et al.⁵⁶

ropy of the ground state polarizability with the applied field. Because TM-BODIPY (Figure 1) belongs to the point group C_{2v} , the electronic transition dipole moment is strictly polarized parallel or perpendicular to the C_2 axis (i.e. the permanent electric dipole axis). The negative value of the coefficient E observed experimentally for TM-BODIPY (see Table 1) shows that the transition dipole direction \hat{m} is perpendicular to the ground-state dipole moment and parallel to the molecular long axis, as is intuitively expected and also predicted by the semiempirical calculations.

For determining the magnitude of the dipole moment, we must estimate the contribution of the anisotropic polarizability (α) in eq 6. This is feasible on the basis of a two-level model⁴⁶ that allows expressing the perturbational contribution to the first optically allowed excited state in terms of the transition dipole moment (μ_{ag}) and the transition wavelength λ_{ag} ,

$$3 \cdot (\hat{m} \cdot \alpha \cdot \hat{m} - \text{Tr} \alpha) = 2\alpha_{yy} - \alpha_{xx} - \alpha_{zz} \approx \frac{4\mu_{\text{ag}}^2 \lambda_{\text{ag}}}{hc} \quad (9)$$

, where h and c have their usual meanings. The value of μ_{ag} can be calculated from the integrated absorption spectrum^{42–45} and λ_{ag} . The latter is taken to be the wavelength of maximum absorption (see Table 1). This estimation leads to a value of 54×10^{-40} $\text{C m}^2 \text{V}^{-1}$ for the left-hand side of eq 9. This corresponds to a polarizability contribution of 131×10^{-20} $\text{C}^2 \text{V}^{-2}$ in eq 6. Now calculating the ground-state dipole moment yields $|\mu| = 10.9 \times 10^{-30}$ C m (=3.3 D).

The value of $\Delta|\mu|$, corresponding to the difference between the excited-state and the ground-state dipoles, is extracted from the coefficients F and G . The dipole moment is perpendicular to the direction of the electronic transition dipole (i.e. $\mu \perp \hat{m}$). Hence, only the difference in polarizability between the excited and ground states contributes to G , which implies a small negative value of the dipole difference (see Table 1). This is within the two-level model qualitatively interpreted as if the energy denominator in the perturbation expression of the polarizability changes sign upon excitation. To calculate the dipole difference from the coefficient F , we assume a negligible

(42) Würthner, F.; Yao, S.; Schilling, J.; Wortmann, R.; Redi-Abshiro, M.; Gallego-Gomez, F.; Meerholz, K. *J. Am. Chem. Soc.* **2001**, in press.

(43) Würthner, F.; Wortmann, R.; Matschiner, R.; Lukaszuk, K.; Meerholz, K.; DeNardin, Y.; Bittner, R.; Bräuchle, C.; Sens, R. *Angew. Chem.* **1997**, *109*, 2933–2936.

(44) Würthner, F.; Wortmann, R.; Matschiner, R.; Lukaszuk, K.; Meerholz, K.; DeNardin, Y.; Bittner, R.; Bräuchle, C.; Sens, R. *Angew. Chem., Int. Ed. Engl.* **1997**, *36*, 2765–2768.

(45) Beckmann, S.; Eitzbach, K.-H.; Krämer, P.; Lukaszuk, K.; Matschiner, R.; Schmidt, A. J.; Schuhmacher, P.; Sens, R.; Seybold, G.; Wortmann, R.; Würthner, F. *Adv. Mater.* **1999**, *11*, 536–541.

(46) Wortmann, R.; Würthner, F.; Sautter, A.; Lukaszuk, K.; Matschiner, R.; Meerholz, K. *Proc. SPIE* **1998**, *3471*, 41–49.

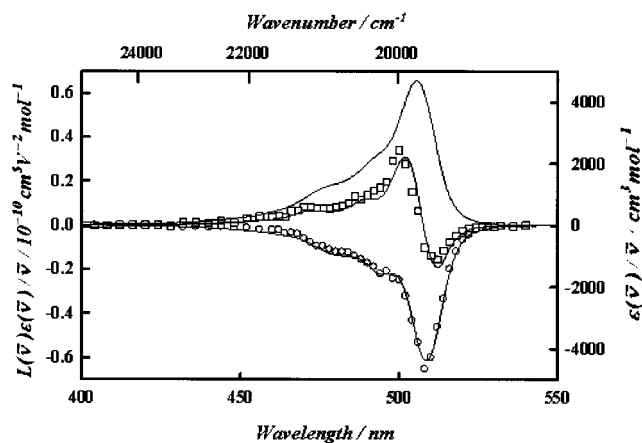


Figure 3. Optical ($\epsilon(\bar{\nu})/\bar{\nu}$, right-hand scale) and electrooptical ($L(\phi, \bar{\nu})\epsilon(\bar{\nu})/\bar{\nu}$, left-hand scale) absorption spectra of BODIPY in dioxane at 298 K. The electrooptical spectra show data points for parallel ($\phi = 0^\circ$, \circ) and perpendicular ($\phi = 90^\circ$, \square) polarization of the light relative to the applied electric field. The solid curves were calculated by multilinear regression.

difference in polarizability perpendicular to the transition dipole. Hence, it is reasonable to approximate the polarizability term of coefficient F in eq 7 according to

$$\text{Tr}\Delta\alpha \approx \hat{m} \cdot \alpha \cdot \hat{m} = \alpha_{yy} \quad (10)$$

and furthermore, to calculate the dipole difference from the difference between F and G . This leads to a small negative value of the dipole difference $\Delta\mu$ given in the Table 1.

According to standard theory, the influence of solvent polarity on absorption spectra of organic dyes^{40,47} yields solvent shifts (“solvatochromism”) proportional to the product of the reaction field (caused by the ground-state dipole moment) and the change of the dipole moment upon electronic excitation. Taken together, the analysis of electrooptical spectra of BODIPY reveals a relatively small ground-state dipole moment and an almost vanishing change of $\Delta\mu$. This explains the exceptionally weak influence from solvent polarity and the microscopic environment on the spectral properties observed for the BODIPY chromophore.

Spectroscopic Properties of BODIPY Groups in the Protein PAI-1. A cysteine substitution mutant of active PAI-1 with unique cysteines in positions 344 and 347 of the reactive center loop was labeled with a sulfhydryl specific BODIPY derivative.¹² As shown in Figure 4, an orbital contact between the two BODIPY moieties is feasible. For this configuration the two molecular planes are located just a few angstroms apart. Such ground- and excited-state dimers were previously reported between Rhodamine B¹⁹ and pyrene,^{48–50} respectively. Indeed the data obtained for BODIPY groups in positions 344 and 347 of PAI-1 show that a ground-state dimer is formed, resulting in the appearance of a new absorption band centered at about 477 nm. Moreover, the shape of the fluorescence spectrum is invariant to excitation in the wavelength region of 450 to 520 nm. In this region the dimer and monomer absorption spectra

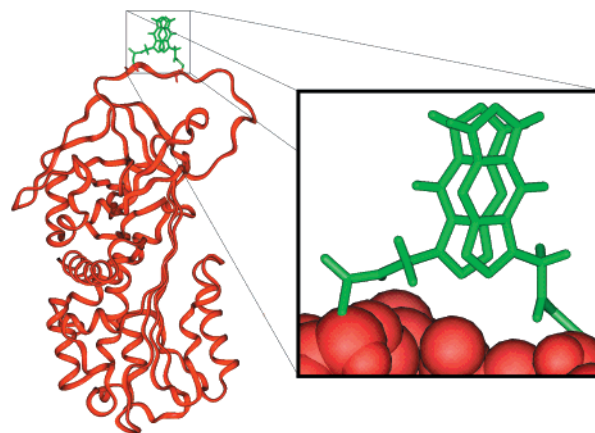


Figure 4. Structure of active plasminogen activator inhibitor, type 1 (PAI-1), as obtained by X-ray crystallography.⁵⁷ Two sulfhydryl specific BODIPY molecules are covalently attached to the S344C and M347C mutated residues. The magnification illustrates one possible conformation of the ground-state BODIPY dimer, for which the molecular planes are parallel and the permanent electric dipole moments are antiparallel. The distance between the molecular planes is 2.7 Å.

are overlapping. This implies that the dimer emission, if at all taking place, is negligible in the region of 500 to 750 nm. Further support is finding that the fluorescence excitation spectra in the presence and absence of dimers are the same as those for pure monomers.

For calculating the dimer absorption spectrum, doubly BODIPY-labeled Cys mutants of active PAI-1 (S344C and M347C, see Materials and Methods) were used. Upon reaction with the urokinase-type plasminogen activator (uPA), the reactive center loop is cleaved between residues 346 and 347. This is followed by a major translocation of one end of the loop resulting in a distance between the two mutated residues of about 60 Å.¹⁴ In active PAI-1 the absorption spectrum is a mixture of the monomer and the dimer spectra, while the spectrum in the cleaved form shows a pure monomer spectrum. To extract the dimer absorption spectrum and the molar absorptivity, quantification of monomer and dimer concentration in active PAI-1 was needed. This was achieved by using the fact that the dimer fluorescence is negligible, which follows from the finding of identical shapes of the fluorescence spectra before and after cleavage of the reactive center loop. The contribution of monomer absorption $\{A_m(\lambda)\}$ in active PAI-1 was determined by measuring the absorption and fluorescence spectra before $\{A_a(\lambda), F_a(\lambda)\}$ and after $\{A_c(\lambda), F_c(\lambda)\}$ cleavage of the PAI-1 reactive center loop. From this the contribution of the monomer absorption was calculated according to

$$A_m(\lambda) = \frac{\Phi_c \int_{\text{band}} F_a(\lambda) d\lambda}{\Phi_a \int_{\text{band}} F_c(\lambda) d\lambda} \left\{ \frac{1 - 10^{-A_c(\lambda_{\text{exc}})}}{1 - 10^{-A_a(\lambda_{\text{exc}})}} \right\} A_a(\lambda) \quad (11)$$

In eq 11, Φ_c and Φ_a denote the fluorescence quantum yield of the monomer in cleaved and active PAI-1, respectively. The ratio Φ_c/Φ_a was taken to be that between the fluorescence lifetime of BODIPY in cleaved and active PAI-1, respectively. Excitation wavelengths (λ_{exc}) were 470 and 480 nm. The dimer molar absorptivity $\{\epsilon_d(\lambda)\}$ was obtained by subtracting the monomer $\{A_m(\lambda)\}$ contribution from the absorption spectrum in active PAI-1 $\{A_a(\lambda)\}$ and dividing by the dimer concentration and the optical path length. For calculating the molar absorp-

(47) Reichardt, W. *Solvents and solvents effects in organic chemistry*; VCH: Weinheim, 1988.

(48) Birks, J. B.; Kazzazz, A. A.; King, T. *Proc. R. Soc., London, Ser. A* **1965**, *291*, 556.

(49) Reynders, P.; Kühnle, W.; Zachariasse, K. A. *J. Phys. Chem.* **1990**, *94*, 4073–4082.

(50) Reynders, P.; Kühnle, W.; Zachariasse, K. A. *J. Am. Chem. Soc.* **1990**, *112*, 3929–3939.

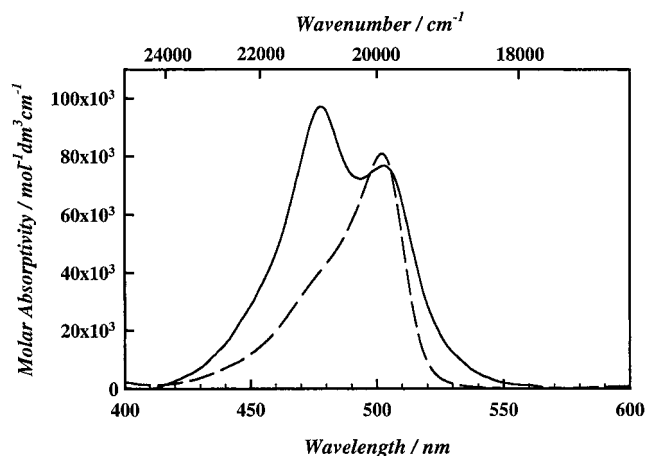


Figure 5. The molar absorptivity of the BODIPY monomer ($\epsilon_m(\tilde{\nu})$, - - -) and dimer ($\epsilon_d(\tilde{\nu})$, —) in double-labeled Cys-mutants of two forms of the plasminogen activator inhibitor type 1 (PAI-1) at 277 K.

tivity, a molar absorptivity of $80\,000\text{ M}^{-1}\text{ cm}^{-1}$ was used for monomeric BODIPY.¹¹

The dimer spectrum (see Figure 5) shows a significantly stronger maximum of molar absorptivity, and it is also broader than the monomer spectrum $\{\epsilon_m(\tilde{\nu})\}$. From a simple theory of exciton coupling within a pair of identical chromophores,⁵¹ the ratio between the integrated absorption spectra of the dimer and the monomer is expected to be 2. We find that the ratio

$$\frac{\int \epsilon_d(\tilde{\nu})\tilde{\nu}^{-1} d\tilde{\nu}}{\int \epsilon_m(\tilde{\nu})\tilde{\nu}^{-1} d\tilde{\nu}} = 1.7 \quad (12)$$

The fluorescence relaxation rate of active as well as cleaved forms of doubly BODIPY-labeled PAI-1 is found to be independent of the excitation wavelength. In both cases the decays are well described by a sum of two exponential functions with a dominating lifetime of 5.8 ns (95%) and a shorter one of about 1 ns. Very similar data are also found for different single BODIPY-labeled mutants of PAI-1.^{5,8,11,52} The reason for a small deviation from monoexponentiality is not known (see Karolin et al.,⁸), but is frequently observed also for other fluorophores that are covalently attached to proteins. As a result of cleaving the bond between the residues 346 and 347, the BODIPY groups become spatially separated by $60 \pm 3\text{ \AA}$.^{12,14} Simultaneously the absorption band centered at about 477 nm disappears, and the fluorescence intensity increases, while the fluorescence lifetimes remain the same. Hence the fluorescence quenching is of the static type, as a result of formation of ground-state dimers. Taken together, the data provide strong evidence for the formation of a ground-state dimer of BODIPY.

Spectroscopic Properties of BODIPY-Labeled Lipids Solubilized in Micelles and DOPC Vesicles. One and two BODIPY groups are covalently bound to residues of sialic acid in the polar headgroups of the gangliosides GM1 and GD1a. Both kind of gangliosides, either nonlabeled or singly or doubly labeled with BODIPY, dissolve at micromolar concentrations in water, whereby micelles are formed.⁵³ The fluorescence

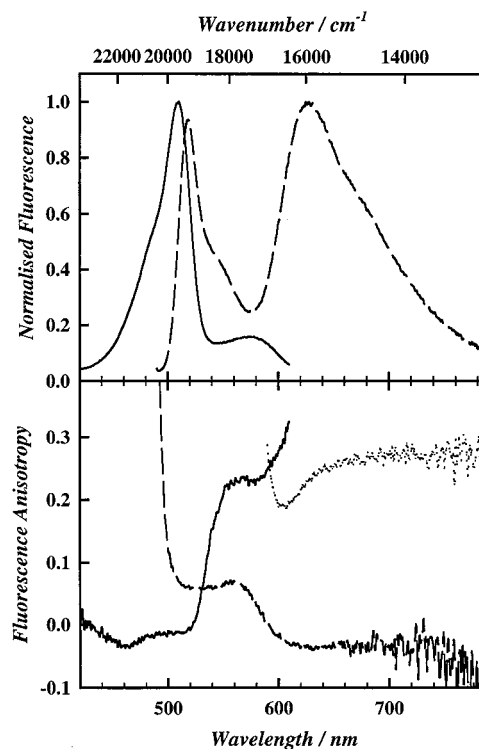


Figure 6. Upper graphs: Emission (- - -, $\lambda_{\text{ex}} = 470\text{ nm}$) and excitation (—, $\lambda_{\text{em}} = 630\text{ nm}$) spectra of bis-BODIPY-labeled ganglioside GD1a in DOPC vesicles at a molar ratio of GD1a:DOPC = 1:50 at 277 K. Lower graphs: Emission (- - -, $\lambda_{\text{ex}} = 470\text{ nm}$; ··· $\lambda_{\text{ex}} = 570\text{ nm}$) and excitation (—, $\lambda_{\text{em}} = 630\text{ nm}$) anisotropy of bis-BODIPY-labeled ganglioside GD1a in DOPC vesicles at a molar ratio of GD1a:DOPC = 1:50 at 277 K.

excitation spectrum of BODIPY reveals a new band located at about 480 nm (data not shown). Interestingly when diluting BODIPY-labeled GD1a with unlabeled GD1a, the fluorescence excitation band at 480 nm decreases, and a band at 570 nm appears. This new band at 570 nm is also observed for BODIPY-labeled GD1a in DOPC vesicles. The absorption bands centered at about 480 and 570 nm strongly support that different ground-state aggregates of BODIPY form. Upon excitation at 470 nm, the fluorescence spectrum reveals a broad emission band centered at about 630 nm in addition to the monomer fluorescence band centered at about 515 nm (Figure 6).

Most likely also the BODIPY-sulfatide (N-BODIPY-FL-pentanoyl-galactosylcerebroside-sulfate)⁵⁴ forms micelles⁵⁵ in water. Absorption spectra recorded at different concentrations of BODIPY-sulfatide show a band located at 484 nm, which resembles the spectrum observed for BODIPY-labeled PAI-1. The fluorescence intensity recorded for BODIPY-sulfatide in water increases up to about $0.13\text{ }\mu\text{M}$, but remains constant at higher concentrations. This suggests a monomeric form of BODIPY-sulfatide below $0.13\text{ }\mu\text{M}$ and the formation of non-fluorescent aggregates of the sulfatide above that value.

Absorption Spectrum of BODIPY Aggregates in Micelles. Assuming dimer formation, the molar absorptivity of BODIPY

- (53) Curatolo, W. *Biochim. Biophys. Acta* **1987**, *906*, 111–136.
 (54) Mikhalyov, I.; Bogen, S.-T.; Johansson, L. B.-Å. *Spectrochim. Acta Part A* **2001**, *57*, 1839–1845.
 (55) Danino, D.; Kaplun, G.; Lindblom, G.; Rilfors, L.; Orådd, G.; Hauksøn, J. B.; Talmon, Y. *Chem. Phys. Lipids* **1997**, *85*, 75.
 (56) Liptay, W.; Becker, J.; Wehning, D.; Lang, W.; Burkhard, O. *Z. Naturforsch.* **1982**, *37a*, 1396–1408.
 (57) Sharp, A. M.; Stein, P. E.; Pannu, N. S.; Carrell, R. W.; Berkenpas, M. B.; Ginsburg, D.; Lawrence, D. A.; Read, R. J. *Structure* **1999**, *7*, 111–118.

(51) Cantor, R. C.; Schimmel, P. R. *Biophysical Chemistry. Part II: Techniques for the Study of Biological Structure and Function*; W. H. Freeman and Company: New York, 1980; Vol. II.

(52) Karolin, J.; Hägglöf, P.; Ny, T.; Johansson, L. B.-Å. *J. Fluorescence* **1997**, *7*, 331–339.

dimers in micelles (data not shown) was determined by using the BODIPY-labeled sulfatide. Samples with lipid concentrations of 0.625 and 2.5 μM ($\text{CMC} = 0.134 \pm 0.017 \mu\text{M}$, unpublished data) were used. The absorption spectra of these solutions exhibit peaks centered at about 484 and 509 nm, indicating a mixture of monomer and dimer spectra. When an excess of sodium dodecyl sulfate (SDS) was added, the micelles were disrupted and the peak at 484 nm disappeared, leaving the pure monomer spectrum of BODIPY. Calculations of the dimer absorption spectrum were performed in the same way as with PAI-1. But instead of using absorption and fluorescence spectra before and after cleavage of the PAI-1 reactive center loop, spectra recorded before and after adding SDS were used. For calculating the molar absorptivity, a molar absorptivity of $80\,000 \text{ M}^{-1} \text{ cm}^{-1}$ was used for monomeric BODIPY.¹¹

Indeed, the extracted spectrum is very similar to that obtained for the BODIPY-dimer in PAI-1. Again using the theory of exciton coupling within a pair of identical chromophores,⁵¹ the ratio between the integrated molar absorptivities of the presumed dimer and the monomer was calculated to be 2.0, which is in perfect agreement with the theoretical prediction (i.e. 2).

Fluorescence Excitation and Emission Anisotropy. The steady-state excitation and emission anisotropies of bis-BODIPY-GD1 solubilized in DOPC vesicles at 277 K are displayed in Figure 6. The steady-state emission anisotropy ($\lambda_{\text{exc}} = 470 \text{ nm}$) is low, about 0.035 in the wavelength region of monomer emission, and also low, about -0.03 , in the region of the 630 band. On the contrary, the emission anisotropy is relatively high (≈ 0.25) for the 630 band, when predominantly aggregates are excited at 570 nm. Upon excitation at about 570 nm a similar value of the excitation anisotropy is obtained for the emission at 630 nm (see Figure 6). This strongly suggests that the broad emission band centered at 630 nm originates from excitation of the ground-state aggregates absorbing at 570 nm.

A nonexponential fluorescence relaxation of BODIPY-lipids in DOPC vesicles (typically at molar ratios higher than 1:100) is observed at 550 nm when exciting at 500 nm. Then the fluorescence relaxation fits well to a sum of two exponential functions. The average fluorescence lifetimes for the different BODIPY-lipids in DOPC decrease with increasing BODIPY concentration, which is compatible with an increased quenching of monomeric BODIPY by the increased formation of BODIPY aggregates.⁵⁴ Also for excitation at 500 and 570 nm, the fluorescence decay at 630 nm is very well described by a sum of two exponential functions, with positive preexponential factors.

BODIPY–BODIPY Interaction in Protein and Lipid Systems. Absorption and fluorescence spectra reveal different aggregation of BODIPY in the double-labeled cystein mutant of active PAI-1, and in lipid phases. In the PAI-1 protein all data are compatible with the formation of a ground-state dimer, which is nonfluorescent. Because the protein concentration is low (μM) there is a negligible intermolecular interaction between BODIPY groups in different protein molecules. The structure of PAI-1 allows the two BODIPY groups to be at distances short enough for an efficient orbital contact. Moreover, the molecular planes can become parallel, as is illustrated in Figure 4. After cleavage of the peptide bond between residues 346 and 347, the ground-state dimer is split into two weakly interacting

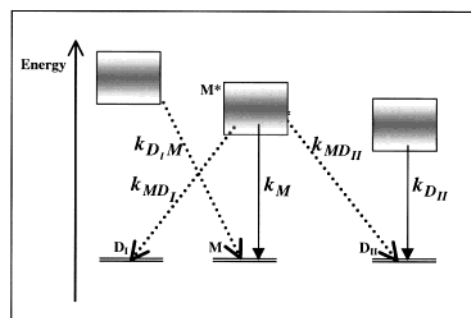


Figure 7. Schematic illustrating different pathways of electronic relaxation for monomeric (M) and two dimeric forms (D_I and D_{II}) of BODIPY.

monomers, as is discussed above in the subsection Spectroscopic Properties of BODIPY Groups in the Protein PAI-1.

The aggregation of the BODIPY lipids is less straightforward to unequivocally interpret. No doubt, however, fluorescent ground-state aggregates are formed. But are these dimers or trimers, etc.? Considering the bulky headgroup of the gangliosides, it is for *steric* reasons likely that no more than two BODIPY moieties can strongly interact. Thus, the formation of ground-state dimers should dominate over higher aggregates.

From the simple theory of exciton coupling between two identical chromophores⁵¹ one can, depending on dimer conformation, expect the appearance of transition bands energetically located below or above that of the monomers. The exciton model is also supported by the ratio of about two found between the integrated dimer and monomer absorption spectra. Within this model the ground-state dimer formed in PAI-1 would correspond to higher energy states (i.e. the 477 nm band), while the long-wavelength transition (at 570 nm) observed in lipid phases represents the lower energy states. The high-energy transition means that the aromatic planes of two BODIPY moieties are preferentially parallel. Hereafter this conformation is referred to as the D_I dimer. Energetic coupling between the permanent dipole moments would lead to a conformation where the C_2 axes of the BODIPY groups are antiparallel. The band at lower transition energy suggests that the molecular planes of BODIPY are located within the same plane with preferentially collinear transition dipoles, hereafter referred to as the D_{II} dimer.

Exciton coupling may lead to a nonvanishing circular dichroism (CD), but no CD was observed for any of the systems showing aggregate absorption. However, the CD effect would vanish for collinear and parallel transition dipoles,⁵¹ or if the orientation distribution of mutually interacting monomers has a 2-fold symmetry about the axis connecting the transition dipole moments. Thus, not observing any CD spectrum is compatible with the proposed conformations of D_I and D_{II} .

Considering all experimental information, some possible photophysical processes for the two dimers and the monomer are summarized in Figure 7. Energy transfer at a rate of k_{MD_I} is expected, as a consequence of overlapping energy gaps between ground and excited states of the monomer and the dimer D_I . The Förster radius of this coupling is estimated to be $57 \pm 2 \text{ \AA}$ (see Materials and Methods). One could then expect that the fluorescence lifetime of the monomer would decrease with increasing concentration of BODIPY lipids in DOPC vesicles, which is indeed observed. Energy transfer from excited D_I to ground-state monomers (at a rate $k_{\text{D}_I\text{M}}$) is also a relaxation path.

Observing excitation spectra that resemble the absorption spectra, i.e. showing a peak at about 480 nm, supports this. On the contrary, because the PAI-1 system examined is diluted (average PAI-1 to PAI-1 distances are on the order of 1000 Å), these processes of energy transfer between monomers and dimers were not observed.

Upon excitation in the region of \mathbf{D}_{II} absorption, an emission band centered at about 630 nm is seen. Thus the excited presumed dimer is fluorescent with an average lifetime of about 3 ns. This interpretation is strongly supported by the very similar values of the excitation and emission anisotropies (see Figure 6). Energy transfer at a rate $k_{MD_{II}}$ may take place from the excited monomer to the ground-state \mathbf{D}_{II} . This is favored by an efficient overlap between monomer fluorescence and the \mathbf{D}_{II} absorption spectra. With excitation in the absorption spectrum of the monomer BODIPY, the red emission band is expected, and is indeed also observed.

Concluding Remarks

Compared to most fluorescent probes the light spectroscopic properties of BODIPY are exceptional. While the electrooptical properties explain the weak solvent dependence on spectra and photophysics of monomeric BODIPY, there is to the best of our knowledge no obvious connection between the electric

properties and the formation of aggregates, such as dimers. It is demonstrated that a presumably sandwich-like dimer (\mathbf{D}_I) can form in a protein as two BODIPY groups are forced into contact. The dimer absorption spectrum is blue-shifted relative to the monomer (\mathbf{M}) spectrum with a peak molar absorptivity of $97000 \pm 7000 \text{ M}^{-1} \text{ cm}^{-1}$ at 477 nm. Electronic energy transfer from the excited \mathbf{M} to \mathbf{D}_I can occur at a rate determined by a Förster radius of $57 \pm 2 \text{ Å}$. Evidence is also given for the occurrence of \mathbf{D}_I at locally high BODIPY concentrations in lipid systems. The dimer \mathbf{D}_I enables new plausible biological and chemical applications, e.g. in studies of protein structure and folding. A second fluorescent ground-state dimer (\mathbf{D}_{II}) is also discovered in lipid phases. An absorption and emission band of \mathbf{D}_{II} is localized at 570 and 630 nm, respectively. In lipid systems \mathbf{D}_I and \mathbf{D}_{II} may co-exist, but \mathbf{D}_I dominates at high local concentrations of BODIPY lipids in water.

Acknowledgment. This work is supported by grants from the Swedish Natural Science Research Council [K650-19981724/2001 (L.B.-Å.J.); B147/199 (T.N.)], the Royal Swedish Academy of Sciences (L.B.-Å.J.), Biotechnical Grants from Umeå University (T.N., L.B.-Å.J.), and the Kempe Foundations (L.B.-Å.J., F.B. and P.H.).

JA010983F